Linear-Hyperbranched Block Copolymers Consisting of Polystyrene and Dendritic Poly(carbosilane) Block

Alejandra García Marcos,[‡] Thomas M. Pusel,[§] Ralf Thomann,[§] Tadeusz Pakula,[†,⊥] Lidia Okrasa,[⊥] Steffen Geppert,[§] Wolfram Gronski,[§] and Holger Frey*[,‡]

Institut für Organische Chemie, Organische und Makromolekulare Chemie, Johannes Gutenberg-Universität Mainz, Duesbergweg 10-14, 55128 Mainz, Germany, Institut für Makromolekulare Chemie, Hermann-Staudinger Haus, Albert-Ludwig Universität Freiburg, Stefan-Meier Strasse 31, 79104 Freiburg, Germany, and Max-Planck-Institute for Polymer Research, Ackermannweg 10, 55128 Mainz, Germany

Received July 13, 2005; Revised Manuscript Received November 28, 2005

ABSTRACT: A general strategy for the preparation of well-defined diblock copolymers combining a random cascade-branched dendritic (i.e., hyperbranched) and a linear block has been developed. The strategy is based on a linear poly(styrene-*b*-butadiene) (PS-*b*-PB) diblock copolymer with high molecular weight PS block and short, functional 1,2-PB block, prepared by conventional anionic polymerization. The functional PB block is used for the grafting of branched AB_2-type carbosilane monomers, resulting in the attachment of a hyperbranched structure to the backbone. Slow addition of the methyldi(undecenyl)silane monomers using Karstedt's catalyst permits control of the molecular weight of the hyperbranched block, resulting in high molecular weight linear-hyperbranched diblock copolymers. Molecular weights of the block copolymers ranged between 72 800 and 106 400 g/mol for M_n, and polydispersity $\bar{M}_w/\bar{M}_n$ was low (typically below 1.1), as predicted by theory for slow monomer addition. Morphological studies by TEM, AFM, and SAXS on these systems demonstrate that various microdomain structures typical for microphase-separated block copolymers can be obtained upon increasing the size of the hyperbranched block with respect to the linear one, despite the strong architectural asymmetry of the linear-hyperbranched macromolecules. However, due to the hyperbranched structure and the crowding of the interface, an asymmetry of the phase diagram is observed. The linear-hyperbranched PS_{520}-*b*-[PB_{47}-*hb*-$PCSi_{142}$] sample with 49 wt % of the hyperbranched component displayed the most unusual morphological behavior

Introduction

In the past decade, block copolymers have attracted increasing scientific and technological interest because of their inherent capability to spontaneously self-assemble into ordered arrays of nanostructures.[1] It is this supramolecular structure formation in bulk or in selective solvents that renders them promising candidates in areas like nanometer-scale patterning of surfaces or encapsulation and release of organic/inorganic compounds, such as drugs.[2] These important applications have fostered the need for well-defined, complex macromolecular architectures. With the development of a variety of controlled synthetic techniques, new macromolecular architectures beyond common segmented structures have been realized.[3] A rich variety of structures has been achieved for example on the basis of linear block copolymers with three distinct block types,[4] blending of linear diblock copolymers,[5] incorporation of rigid rodlike segments,[6] introduction of liquid crystallinity,[7] and attachment of dendrons to a polymeric core in the so-called "dendronized polymers"[8] or more recently by the preparation of nonlinear block copolymers.[9]

Within nonlinear block copolymer systems containing cascade-branched blocks, several groups have focused on AB-diblock structures consisting of a linear and a dendrimer block, showing some peculiar properties of such materials.[10] However, the preparation of a perfectly branched dendron block represents a time-consuming multistep synthesis. In addition, the size of the dendrimer block is limited to the respective perfect dendrimer generation. While there is a considerable number of publications devoted to the preparation and characterization of these linear−dendritic architectures,[10a] very little literature exists concerning solid-state or thin film properties.[11]

In the current paper, we describe a strategy for the preparation of novel linear-hyperbranched diblock copolymers with narrow polydispersities, based on the grafting of branching monomers onto a linear diblock template structure.[12] If suitable monomers are employed, this so-called "hypergrafting" strategy leads to an unusual class of polymer brushes with dendritic molecular architecture. To generate linear-hyperbranched diblock copolymers, a long linear A_n block is combined with a short polyfunctional B_f-type structure that acts as a core for the ensuing hypergrafting procedure. In a second "pseudo-chain growth" step, suitably designed AB_2-monomers are grafted onto the B_f block (Figure 1).

The "hypergrafting" concept has been applied to an anionically synthesized polystyrene-*block*-poly(1,2-butadiene) diblock copolymer (PS_x-*b*-PB_y),[13] using methyldiundec-10-enylsilane[14] as an AB_2 monomer in a hydrosilylation type reaction (Figure 1). This monomer was chosen because it is plausible that the long alkyl chain would reduce the likelihood of an intramolecular cyclization reaction of the focal group of the growing hyperbranched polymers. Hence, block copolymers with a well-defined, linear polystyrene block and a highly flexible, hyperbranched polycarbosilane block are obtained. Catalytic hydrosilylation[15] has been chosen as a synthetic route for "hypergrafting" of the vinyl groups of the short PB block, since it is a high conversion transformation. In this manner a hyperbranched,

† Deceased.
‡ Johannes Gutenberg-Universität Mainz.
§ Albert-Ludwig Universität Freiburg.
⊥ Max-Planck-Institute for Polymer Research, Ackermannweg 10, 55128 Mainz, Germany.
* Corresponding author. E-mail: hfrey@uni-mainz.de.

10.1021/ma051526c CCC: $33.50
Published on Web 01/11/2006

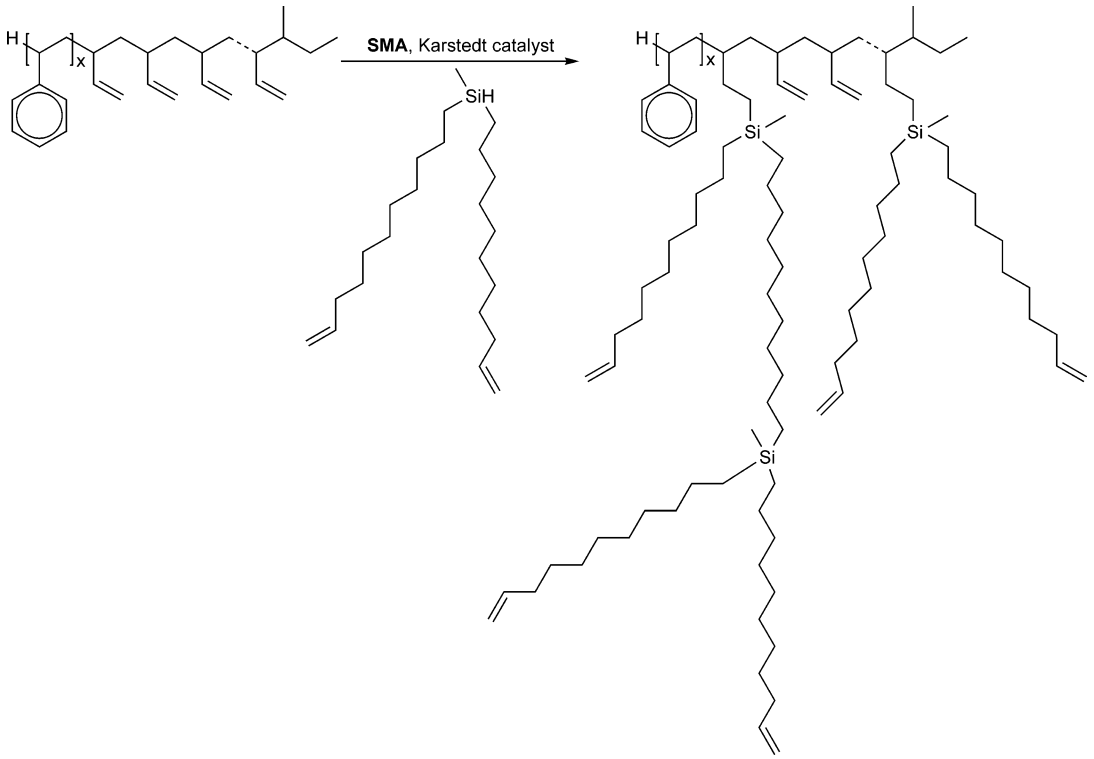

Figure 1. Synthesis of linear-hyperbranched block copolymers by grafting of branched AB_2 carbosilane monomers on a short polybutadiene (PB) block of PS_x-*b*-PB_y.

polyethylene-like block incorporating highly flexible polycarbosilane branches is obtained. In this paper, we detail the synthesis of a series of linear-hyperbranched diblock copolymers prepared via this route, systematically varying the molecular weight of the hyperbranched block. Furthermore, the results of a detailed investigation of the structures resulting from nanophase-segregation of such block copolymers will be given, using TEM, AFM as well as scattering methods.

Materials and Methods

Nomenclature. Polystyrene-*block*-poly(1,2-butadiene) diblock copolymers are designated PS_x-*b*-PB_y, in which *x* indicates the degree of polymerization (DP_n) of the PS block and *y* the DP_n of the 1,2-PB block. Hyperbranched-linear diblock copolymers are denoted by PS_x-*b*-[PB_y-*hb*-$PCSi_z$], in which *y* indicates the DP_n of 1,2-PB and *z* the DP_n of the polycarbosilane block (PCSi). The hyperbranched block formed after grafting of the branched carbosilane monomers is designated [PB_y-*hb*-$PCSi_z$], since the short 1,2-PB block is regarded as part of the final PCSi block.

General Information. Solution ^{1}H NMR, ^{13}C NMR and ^{29}Si NMR spectra were recorded on a 300 or 400 MHz (Bruker) spectrometer in $CDCl_3$. Gel permeation chromatography (SEC) measurements were performed in chloroform using a column combination of $10^6-10^5-10^4$ Å or $10^4-10^3-10^2$ Å from PSS Co. Membrane osmometry (MO) was carried out using an Osmomat 090 membrane osmometer in toluene at 40 °C in a concentration range of 10−70 mg/mL. DSC measurements (heating and cooling rates of 25 °C/min) were performed on a Perkin-Elmer 7 in the temperature range of −100 to +150 °C, and the melting point of indium (156 °C) was used for calibration. For TEM characterization, we utilized melt-pressed samples as well as solid films ∼5 mm thick that were slowly cast at room temperature (ca. 3 weeks and a week under vacuum to remove residual solvent) from ca. 5 wt % polymer solutions in toluene. The samples were then annealed for ca. 2 h under high vacuum at 150 °C. TEM experiments were carried out with a LEO 912 Omega transmission electron microscope applying an acceleration voltage of 120 keV. The specimens were prepared using a Leica ULTRACUT UCT ultramicrotome equipped with a cryo-chamber. Thin sections of about 50 nm were cut with a Diatome diamond knife at −120 °C. The samples were measured without RuO_4 staining. AFM experiments were performed with a Nanoscope III scanning probe microscope. Height and phase images were obtained simultaneously, while operating the instrument in the tapping mode under ambient conditions. Images were taken at the fundamental resonance frequency of the Si cantilevers, which was typically around 180 kHz. Typical scan speeds during recording were 0.3−1 line/s using scan heads with a maximum range of 16 × 16 μm. The flat surfaces of the samples examined, were obtained by cutting with a Diatome diamond knife at −120 °C using a Leica ULTRACUT UCT ultramicrotome equipped with a cryo-chamber. SAXS experiments were performed. SAXS measurements were conducted using a rotating anode (Rigaku 18 kW) X-ray beam with a pinhole collimation and a two-dimensional detector (Bruker) with 1024 × 1024 pixels. A double graphite monochromator for the Cu Kα radiation (λ = 0.154 nm) was used. The beam diameter was about 0.5 mm and the sample to detector distance was 1.3 m. The recorded 2D scattered intensity distributions were integrated over the azimuthal angle and are presented as functions of the scattering vector ($s = 2\sin\theta/\lambda$, where 2θ is the scattering angle). Samples in the form of 1 mm thick plates were prepared by press molding at a temperature of 140 °C. Measurements at various temperatures were performed after subsequent heating steps between room temperature and 200 °C and after final cooling to room temperature (30 °C) as well.

Materials. PS_x-*b*-PB_y, with a 100% 1,2-PB content, was prepared in 20 g amounts via a simplified anionic polymerization procedure according to Sänger et al.,[13] using a specially constructed reactor system suitable for working under high vacuum and overpressure. Methyldiundec-10-enylsilane was synthesized according to described literature procedures. For the hypergrafting reaction, *cis,trans*-decahydronaphthalene (Aldrich; anhydrous; >99%) was used as received and *n*-pentane (Fischer Scientific; p.a.) distilled over sodium before use. Platinum-divinyltetramethyldisiloxane complex in xylene (ABCR; 3−3.5% platinum) was used as the hydrosilylation catalyst.

Synthesis of PS_{520}-*b*-[PB_{47}-*hb*-$PCSi_{76}$]. The polymer-analogous hydrosilylation reaction was carried out under argon atmosphere.

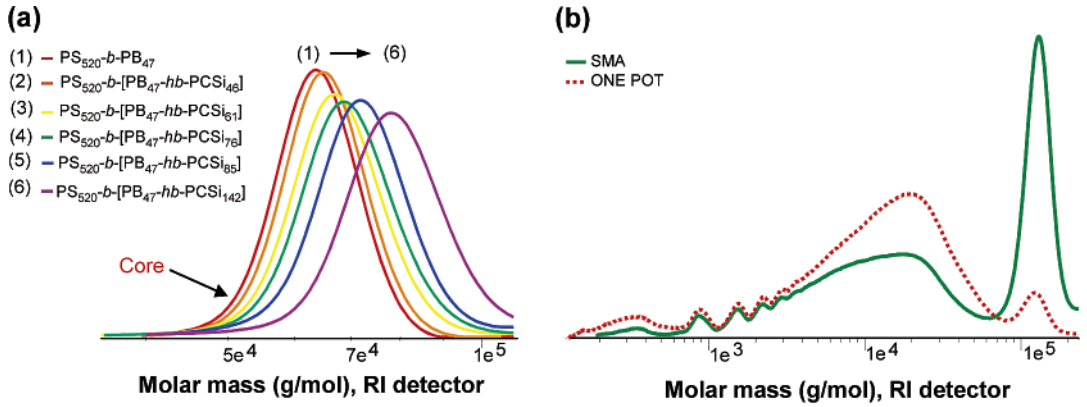

Figure 2. (a) SEC diagrams of the linear core (PS_{520}-*b*-PB_{47}, M_n = 63 800 g/mol) and the linear-hyperbranched block copolymers with increasing amount of added MDUS (AB_2 monomer). (b) SEC diagrams for comparison of a hypergrafting reaction carried out in one-pot and SMA mode for sample PS_{1166}-*b*-PB_{118} (M_n = 118 000 g/mol).

Methyldiundec-10-enylsilane (1.75 g, 5 mmol) was dissolved in pentane (350 mL) and slowly added via a dosing pump to a solution of the diblock copolymer PS_{520}-*b*-PB_{47} (1 g, 0.83 mmol PB) in *cis,trans*-decaline (15 mL) at 70 °C containing 0.01 mmol of Karstedt's catalyst. Pentane was removed by distillation during the slow addition of the monomer. The polymer PS_{520}-*b*-[PB_{47}-*hb*-$PCSi_{76}$] was purified by fractionating precipitation. This was achieved by diluting the decaline reaction mixture with diethyl ether (ca. 150 mL), followed by the dropwise addition of methanol until the polymer precipitated. The supernatant fluid was decanted and the precipitate was washed several times with methanol and dried in vacuo at 40 °C. For the synthesis of the analogous polymer PS_{520}-*b*-[PB_{47}-*hb*-$PCSi_z$], the quantity of monomer added was gradually increased, so that the molar quantity of the monomer was at least equal to the molar quantity of the 1,2-PB core. A polymer with a number-average molecular weight (M_n) of 83 400 g/mol and with a polydispersity index (PDI) of 1.05 was obtained as determined by membrane osmometry (MO) and SEC measurements, respectively. The analogous one-pot reaction was carried out by adding the neat monomer directly to a solution of the diblock copolymer in decaline and heating at 70 °C for 24 h.

^{1}H NMR (400 MHz, $CDCl_3$): δ (ppm) 7.4−6.7 (m, C_6H_5), 5.9 (m, C**H** = CH_2, PCSi), 5.7−5.3 (m, −C**H**=C**H**−, PCSi; C**H**=CH_2, PB), 5.1−4.8 (m, CH=C**H**$_2$, PB, PCSi), 2.4−0.8 (polymer backbone), 0.51 (−Si−CH_2), −0.05 (Si−CH_3). ^{13}C NMR (75 MHz, $CDCl_3$): δ (ppm) 146−145, 139.5, 132, 130−125, 124.8, 114.4, 47−38, 36.6, 34.6, 34.2, 33, 30.5−29, 27, 24.2, 18.3, 14.2, −4.8. ^{29}Si NMR (60 MHz, $CDCl_3$): δ (ppm) 2.9. IR: γ(cm^{-1}) 3103, 3081, 3059, 3025, 2919, 2850, 1601, 1583, 1492, 1451, 1366, 1248, 1181, 1155, 1069, 1028, 965, 907, 755, 696, 539.

Results and Discussion

From a theoretical point of view, the synthesis of the desired polystyrene-*b*-(*hb*-polycarbosilane) block copolymers can be carried out either by slow addition of the AB_2-type carbosilane monomers to the linear block copolymer precursor or in a one pot procedure, simply adding the Pt-catalyst to a mixture of the block copolymer precursor and the carbosilane monomer. In the case of the slow monomer addition, a dilute solution of the dialkenyl silane monomer was slowly added (12−36 h) to a concentrated solution of the diblock copolymer in decaline in the presence of the Karstedt catalyst.[16] The amount of silane monomer used depended on the desired molecular weight of the hyperbranched block. SEC analysis of the crude reaction product showed a bimodal molecular weight distribution. The undesired broad low molecular weight-fraction ($\bar{M}_w/\bar{M}_n \sim 3.0$) corresponds to AB_2 monomers polymerized via a step-growth mechanism, generating low molecular weight hyperbranched homopolymers, which can eventually cyclize and therefore are not attached to the growing branched diblock structure. However, utilizing the solubility characteristics of the large PS block, these nonattached hyperbranched polycarbosilane homopolymers were conveniently separated from the desired diblock copolymers by fractionating precipitation in diethyl ether/methanol. The high molecular weight mode of the molecular weight distribution is clearly due to the desired grafted block copolymer. Grafting of the hyperbranched block via the slow monomer addition (SMA) strategy[17] allows "pseudo chain growth" kinetics to be achieved. Although the SMA does not proceed in an ideal manner (i.e., complete attachment of the branched monomers to the chain is not achieved), the molecular weight of the resulting linear-hyperbranched polycarbosilane block copolymers increases linearly with the amount of AB_2 monomer added (Figure 2a). Hence, very narrow molecular weight distributions were obtained for the grafted block copolymers ($\bar{M}_w/\bar{M}_n$ = 1.04−1.25) and the characteristics of a controlled polymerization appear to be fulfilled. A comparison of the SEC results of the one-pot procedure with slow monomer addition is instructive with respect to the advantages of slow monomer addition. Clearly, grafting reactions carried out via SMA resulted in considerably lower formation of hyperbranched homopolymer than polymerizations performed in one-pot procedures, as clearly seen from the relative intensities of the two modes (Figure 2b). As expected, the intensity of the broad, lower molecular weight mode due to hyperbranched polycarbosilane homopolymer not attached to the linear polymer backbone is considerably higher in the case of the one-pot procedure. It is reasonable to assume that the hyperbranched carbosilane is present in a cyclized form. This reaction of the focal SiH unit prevents further attachment to the block copolymers. However, it should be emphasized that there is no possibility to support cyclization by additional evidence, since mass spectroscopy cannot distinguish between the hyperbranched and the cyclic species.

In the ^{1}H NMR spectrum of the linear diblock (Figure S1, Supporting Information), two broad signals are observed in the olefinic region at δ = 5.5 and 5.0 ppm in the ratio 1:2. These correspond to the methine and methylene protons, respectively, of the polybutadiene vinyl groups. After hypergrafting, the ^{1}H NMR spectrum exhibits three signals in the olefinic region. A relatively sharp new signal appears at δ = 5.9 ppm, assignable to the methine protons of the pendant carbosilane vinyl groups, which are denoted by "e" in Figure 3. The signal at δ = 5.0 ppm is ascribed to the vinyl methylene protons of the carbosilane units (signal "d") and the methylene protons (signal "a") of the unreacted polybutadiene vinyl groups. The methine protons of the unreacted butadiene units (signal "b") again give rise to a very broad signal between 5.7 and 5.3 ppm with an additional

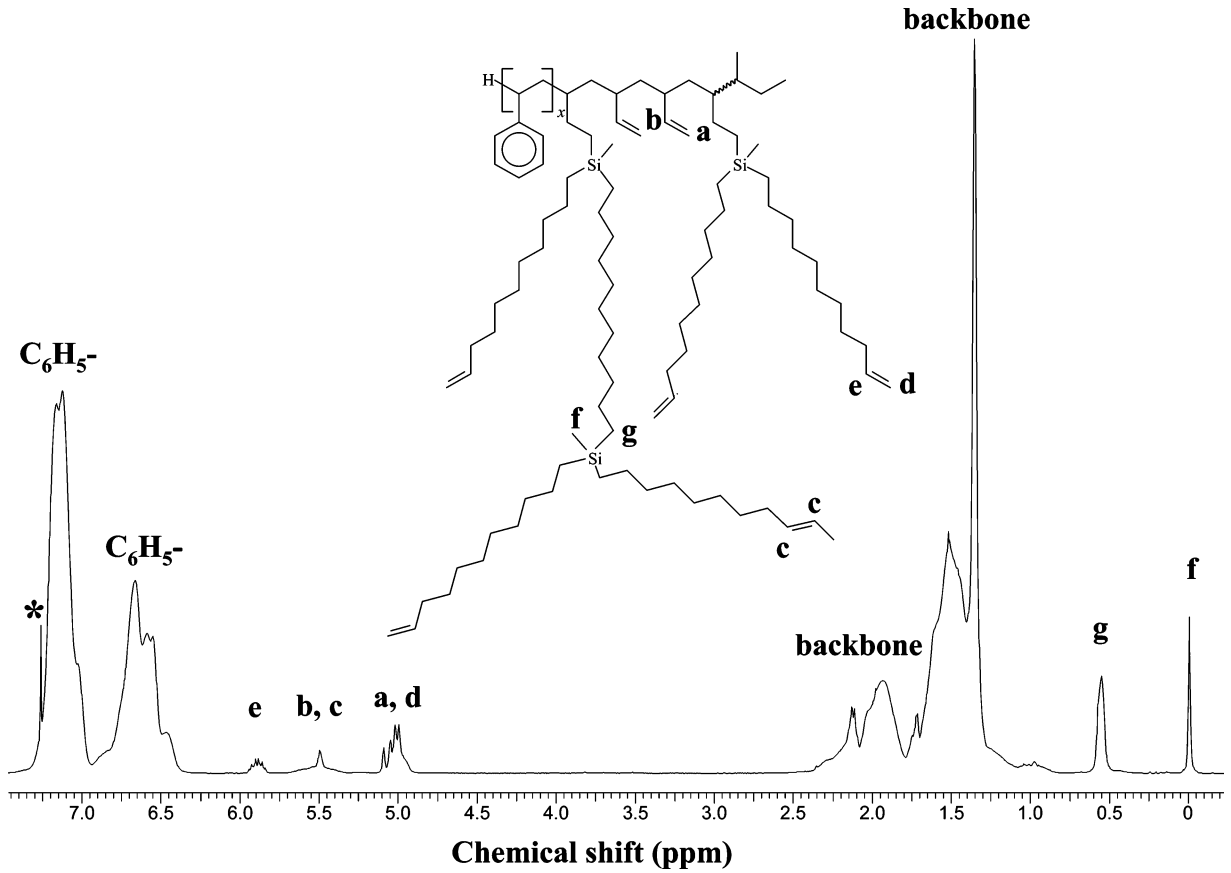

Figure 3. ^{1}H NMR spectrum of PS_{520}-*b*-[PB_{47}-*hb*-$PCSi_{76}$] (solvent peak denoted by an asterisk).

sharp peak at $\delta = 5.0$ ppm. Examination of the ^{1}H−^{1}H COSY spectrum (Figure S2, Supporting Information) reveals that the sharp signal at $\delta = 5.5$ ppm exhibits no coupling within the olefinic region and we therefore assign this to the isomerized protons of the carbosilane groups labeled "c". Only one signal was found in the ^{29}Si NMR spectrum of the PS_{520}-*b*-[PB_{47}-*hb*-$PCSi_z$] samples, which is consistent with the exclusive formation of the anti-Markovnikov addition product (Figure S3, Supporting Information). Moreover, this negates the possibility to determine the degree of branching. In other words, the long C_{11} alkyl chains, resulting in a large distance between the branching centers do not permit to distinguish the different possible types of silicon units (i.e. branched, linear and terminal).

Obviously, the formation of hyperbranched homopolymer, formally representing a new (B_m-type) core molecule, is a consequence of the increased monomer concentration in the reaction mixture during the hypergrafting process, which results in competition between the chain-growth and the step-growth mechanisms. There are several contributing factors that could explain this: (i) steric factors, i.e., the large PS block in the PS-*b*-PB block copolymer, retards the polymer-analogue hydrosilylation reaction, when compared to pure PB;[18] (ii) analysis of the ^{1}H NMR spectra of the linear-hyperbranched PS-*b*-polycarbosilanes reveals that during the reaction nonreactive internal double bonds are formed by double bond isomerization;[19] (iii) the reactivity of the methyldiundec-10-enylsilane monomer can be considered to be relatively low due to the absence of electron-withdrawing groups that expedite the formation of the intermediate Si−Pt complex;[20] (iv) attachment of the catalytic species to the more flexible, nonbulky double bonds of the hyperbranched polycarbosilane homopolymer may be favored. Characterization data for the linear diblock copolymer (PS_{520}-*b*-PB_{47}) containing 4.5 wt % of PB and for all

Table 1. Characterization Data and Thermal Properties for the Linear (PS_x-*b*-PB_y) and the Respective Linear-Hyperbranched Diblock Copolymers (PS_x-*b*-[PB_y-*hb*-$PCSi_z$])

	SEC[a]		MO[b]		DSC	
sample	M_n (10^3 g/mol)	PDI[c]	M_n (10^3 g/mol)	wt % PS	T_{g_1} (°C)	T_{g_2} (°C)
PS_{520}-*b*-PB_{47}	63.8	1.04	56.8	95.5	99.7	−48.6
PS_{520}-*b*-[PB_{47}-*hb*-$PCSi_{46}$]	65.2	1.06	72.8	75	88.2	−24.7
PS_{520}-*b*-[PB_{47}-*hb*-$PCSi_{61}$]	67.8	1.04	78.0	70	93.4	−42.2
PS_{520}-*b*-[PB_{47}-*hb*-$PCSi_{76}$]	69.6	1.05	83.4	65	87.0	−31.0
PS_{520}-*b*-[PB_{47}-*hb*-$PCSi_{85}$]	80.7	1.25	86.7	63	96.0	−61.1
PS_{520}-*b*-[PB_{47}-*hb*-$PCSi_{142}$]	86.0	1.13	106.4	51	101.7	−68.6

[a] Gel permeation chromatography measured in chloroform with PS standard calibration. [b] Membrane osmometry measured in toluene at 40 °C. [c] Polydispersity index $\bar{M}_w/\bar{M}_n$.

resulting linear-hyperbranched polycarbosilane structures PS_{520}-*b*-[PB_y-*hb*-$PCSi_z$] are summarized in Table 1. In the linear-hyperbranched block copolymers the short PB block becomes a part of the final polycarbosilane block and is also treated as such in all ensuing considerations. This is justified by the fact that the PB core in the final linear-hyperbranched architectures is indistinguishable from the grafted carbosilane units. Not represented in Figure 2, the SEC curves of the polymers exhibit a trace mode at high molecular weights that may result from oxygen-induced dimerization of a small fraction of the PS-*b*-PB copolymers during anionic polymerization (Figure S4, Supporting Information). The polydispersity values presented include this high molecular weight mode. As expected, the molecular weights of the hyperbranched block copolymer structures, as determined by conventional SEC (polystyrene standards), are underestimated. For instance, for PS_{520}-*b*-[PB_{47}-*hb*-$PCSi_{142}$] SEC-measurements give an M_n value of 86 000 g/mol, whereas MO results in an absolute molecular weight of 106 400 g/mol, illustrating the effect of the compact, hyper-

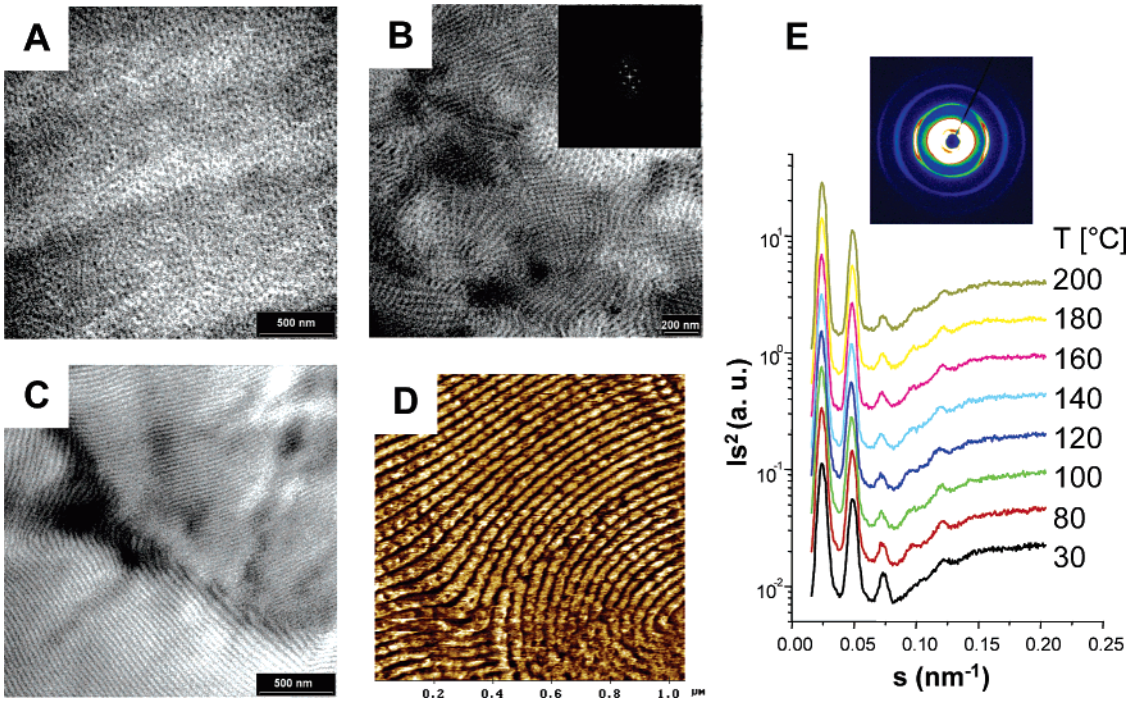

Figure 4. Unstained TEM (silicon contrast) (A, B, and C), AFM phase image (D) and SAXS (E) of the linear PS (bright areas) hyperbranched polycarbosilanes (dark areas): (A) PS_{520}-*b*-[PB_{47}-*hb*-$PCSi_{46}$], (B) PS_{520}-*b*-[PB_{47}-*hb*-$PCSi_{76}$] and FT of PS_{520}-*b*-[PB_{47}-*hb*-$PCSi_{61}$], (C and D) PS_{520}-*b*-[PB_{47}-*hb*-$PCSi_{85}$], and (E) PS_{520}-*b*-[PB_{47}-*hb*-$PCSi_{85}$] one- and two-dimensional SAXS pattern illustrating long-range lamellar order.

branched structure of the polycarbosilane block. The weight percentage of PS and PB, respectively, in the linear core was calculated from the ^{1}H NMR spectra, while absolute molecular weights were determined using membrane osmometry (MO). The wt % of the linear PS and the hyperbranched [PB-*hb*-PCSi] blocks was calculated from MO data for each sample.

Besides establishing a synthetic route for linear-hyperbranched block copolymers, the main objective of this study was to examine the influence of the branched topology on the bulk morphology, when compared to common linear diblock copolymer systems. Considering the large number of topological isomers even for species of the same molecular weight, it appeared intriguing to study the possibility of supramolecular ordering. The thermal behavior of the polymers was investigated using differential scanning calorimetry (DSC). All linear-hyperbranched block copolymers exhibit two glass transition temperatures (T_g), which indicates microphase segregation in the bulk state. Clearly, grafting of the branched carbosilane monomer on the PB block does not lead to reduced flexibility, in contrast to dendronized polymers, illustrating the difference between the random branching pattern present in such "hyper-grafted" materials and the perfectly branched side group structure of dendronized polymers that leads to rigidification as a consequence of steric crowding.[8] Characterization of the resulting bulk morphologies was accomplished by atomic force microscopy (AFM), transmission electron microscopy (TEM), and temperature-dependent small-angle X-ray scattering (SAXS) measurements. SAXS patterns were obtained from melt-pressed samples, while AFM and TEM images were taken from both melt-pressed and solution-cast films in toluene, a nonpreferential solvent. However, the observed morphologies were largely independent of the sample pretreatment, the only difference being that the solution-cast films displayed a higher degree of order than the melt-processed samples. Generally, the contrast in the TEM images is based solely on differences in electron density between silicon and carbon, in other words, no additional staining has been applied.

A TEM micrograph of sample PS_{520}-*b*-[PB_{47}-*hb*-$PCSi_{46}$] containing 25 wt % of the hyperbranched block (HB) is shown in Figure 4A. In the case of a linear diblock copolymer with similar wt % fractions, formation of cylinders at the strong segregation limit (SSL) is expected. Nevertheless, the micrograph shows rather irregular [PB-*hb*-PCSi] domains dispersed in the PS matrix with no discernible lattice. Also, the corresponding SAXS patterns recorded up to 200 °C do not fit exactly to a hexagonally packed cylindrical morphology. The scattering curve displays an intense, but broad scattering peak at the scattering vector (s^*) with only a weak second order broad peak, resembling patterns from nearest neighbor correlated arrangements of domains without a specific shape. This suggests that this sample may not be within the strongly phase-segregated regime.[1] It is also possible, that this disordered morphology is related to the "wormlike micelle" morphology found by Gido et al. for a I_2S graft block copolymer having 81% volume fraction of the styrene block.[21] Disordered cylinders or little ordered "wormlike" structures are not uncommon at the limits of segregation in linear systems of similar composition.

Samples PS_{520}-*b*-[PB_{47}-*hb*-$PCSi_{61}$] and PS_{520}-*b*-[PB_{47}-*hb*-$PCSi_{76}$] with 30 and 35 wt % HB, respectively, show cylindrical morphology (Figure 4B). The TEM for the sample PS_{520}-*b*-[PB_{47}-*hb*-$PCSi_{61}$] demonstrated hexagonally packed cylinders with long-range order as evidenced by a Fourier transformation of the TEM micrograph (inset Figure 4B). The regularly ordered packing of the [PB-*hb*-PCSi] domains is consistent with the X-ray diffraction patterns for both samples. The SAXS intensity distributions exhibit three reflections at s^*, $2s^*$ and $s^*\sqrt{7}$, which corresponds to cylinders packed in hexagonal arrays with domain periodicities (d) of 35 and 39 nm, respectively. Annealing of the sample above the T_g of PS (200 °C) causes the intensity of the third Bragg peak to become sharper and reflects the increased order and more uniform phase separation.

A clear lamellar phase was found for the sample PS_{520}-*b*-[PB_{47}-*hb*-$PCSi_{85}$], which contains 37 wt % of the HB component (Figure 4, parts C and D). This morphology is also expected in

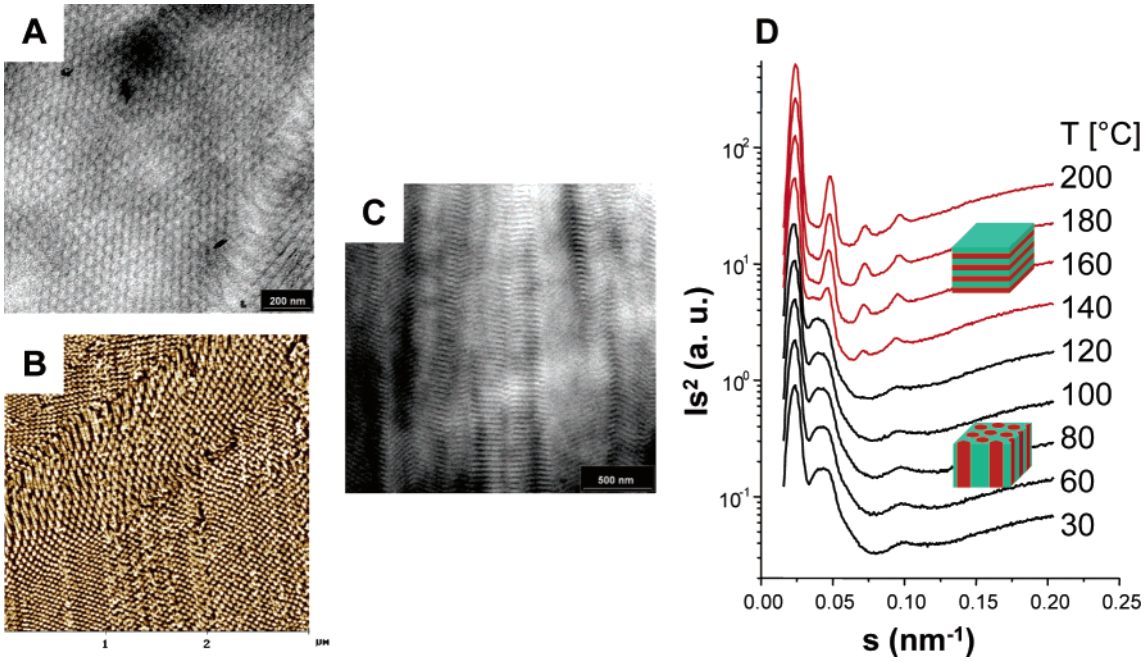

Figure 5. Morphology studies of sample PS_{520}-*b*-[PB_{47}-*hb*-$PCSi_{142}$]: (A and B) unstained TEM and AFM phase image at room temperature from the melt-pressed sample, (C) TEM at room temperature from the solution-cast sample, and (D) temperature-dependent one-dimensional SAXS pattern.

the SSL for linear diblock copolymers with similar composition. In the TEM picture we see how the lamellae are ordered in different grains. The sample exhibits well-developed order and as a result SAXS reflections up to the fifth order are detected. The corresponding SAXS pattern and related intensity distribution is presented in Figure 4E, from which a lamellar long period of 42 nm is determined.

Except for the first linear-hyperbranched sample PS_{520}-*b*-[PB_{47}-*hb*-$PCSi_{46}$], we assume that these systems are within the SSL, because no order−disorder transition was observed prior to heating in the SAXS experiments (Figure 4E). Moreover the samples showed high order after only 2 h of annealing above the T_g of PS, indicating a rapid ordering process. The fact that the materials displayed in general long-range periodicity is indicative of well-defined monodisperse samples.[1] Microstructures detected in the studied samples were maintained in the melt up to temperatures far above the glass transition temperature of PS (up to 200 °C). Moreover, long-range order appeared to improve by heating the sample. This indicates well-stabilized structures characteristic of the strong segregation range. This is unusual, since the interaction parameter (χ_{AB}) usually varies inversely with temperature,[4] i.e., miscibility is improved as the temperature rises. We presume that a large entropic factor must contribute to the conformational asymmetry existing between the dendritic and the linear blocks (as also noted by Pochan et al. and Mackay et al.),[11] making the blocks less compatible. Most probably a limited penetrability of the hyperbranched [PB-*hb*-PCSi] blocks by linear PS chains is responsible for this entropic contribution and constitutes a strong component of the driving force for the microphase separation.

The linear-hyperbranched PS_{520}-*b*-[PB_{47}-*hb*-$PCSi_{142}$] sample with 49 wt % of the hyperbranched component displayed the most unusual morphological behavior (Figure 5). Hexagonally packed PS cylinders in a [PB-*hb*-PCSi] matrix can be observed for the melt-pressed sample as demonstrated by TEM (Figure 5A) and AFM images (Figure 5B). The SAXS intensity distributions (Figure 5D) display the reflections typical of a cylindrical morphology with d of 50.4 nm up to 120 °C. However, above this temperature the morphology pattern unexpectedly changes to a lamellar-like structure with a lamellar period of 40.5 nm. The morphology change observed upon heating was reproducible, but not reversible. In other words, when the samples were cooled slowly the lamellar morphology remained. It can be supposed that the cylindrical structure detected initially can be formed during sample deformation, but when annealed it transforms to a lamellar morphology characteristic as the equilibrium state at this molecular composition. The lamellar phase can be recognized also in the TEM picture of the solution-cast sample (Figure 5C), which agrees with the SAXS patterns obtained above the T_g of PS. Taking into account the studies of miktoarm star block copolymers,[22] one could speculate that because of the strong architectural asymmetry between the linear and hyperbranched blocks, even at the comparable weight fractions of both components, a local preferential curvature of the PS-*b*-[PB-*hb*-PCSi] interface can be formed. In such a case, patterns other than lamellar morphologies would be formed in contrast to linear diblock copolymers of comparable composition for which a lamellar morphology is expected.[4] The results for the studied samples do not confirm such a conjecture. Determination of the complete phase diagram for the studied system would, however, require samples well distributed over the composition scale. On the basis of these results, we can surmise that the interface is forced to curve toward the PS system only under deformation. This is probably due to an overcrowding of the hyperbranched blocks, forcing PS domains to assume cylindrical forms. Such a structure becomes unstable at high temperatures and in solution where the higher chain mobility allows an irreversible relaxation to the equilibrium morphology.

Conclusion

In summary, an innovative strategy for the preparation of linear-hyperbranched block copolymers based on slow monomer addition to a linear block copolymer precursor has been developed, which permits control of the molecular weight of the hyperbranched block, while keeping the apparent polydis-

persity of the materials low (almost always $\bar{M}_w/\bar{M}_n < 1.1$). In a recent paper, we have confirmed the general validity of this approach by the preparation of amphiphilic linear-hyperbranched block copolymers.[23] In this work we have been able to demonstrate—to the best of our knowledge for the first time[12]—that linear-hyperbranched polymers are capable of forming highly ordered nanophase-segregated morphologies, despite additional structural isomerism of the branched block in addition to the polydispersity regarding molecular weight. Manipulation of the composition of these novel materials allows morphological control analogous to that in linear diblock copolymers. Despite the structural asymmetry between the blocks, microphase-separated states similar to those observed for linear diblock copolymers were detected. Phase segregation persists above the T_g of polystyrene up to the decomposition temperature of the materials, and even at elevated temperatures highly ordered, phase-segregated structures were observed, indicative of the very strong segregation.

The branched structure appears to represent a topological contribution to the incompatibility and the resulting order, i.e., cylindrical structures were observed for the sample PS_{520}-*b*-[PB_{47}-*hb*-$PCSi_{142}$] with 49 wt % of the hyperbranched component. However, after annealing an irreversible transformation to the expected lamellar structure took place. Thus, the cylindrical morphology is likely to represent a kinetically controlled or metastable state and does not represent an equilibrium morphology.

Further studies are in progress in order to construct a precise phase diagram for a comprehensive comparison of the structure-morphology relationship of such copolymers with established linear and branched copolymer architectures.

Acknowledgment. We thank Margarete Deptolla, Heidi Wisser, and Carola Sturm for their technical assistance. We are grateful to Prof. Finkelmann and the Institut für Makromolekulare Chemie in Freiburg for the use of the membrane osmometer. Special thanks to Prof. Thomas Thurn-Albrecht for his collaboration in the early stage of the project. Furthermore, we thank Dr. Andreas Kilbinger, Dr. Alexander Theis, and Dr. Tony Farrell for helpful discussions in preparing this manuscript. H.F. acknowledges support from the Fonds der Chemischen Industrie (FCI).

Supporting Information Available: Figures showing the ^{1}H NMR spectrum of PS_{520}-*b*-PB_{47} (Figure S1), a ^{1}H−^{1}H COSY NMR spectrum of PS_{520}-*b*-[PB_{47}-*hb*-$PCSi_{76}$] (Figure S2), and a ^{29}Si NMR spectrum of a typical block copolymer (Figure S3) as well as GPC chromatogram of PS_{520}-*b*-[PB_{47}-*hb*-$PCSi_{76}$] (Figure S4). This material is available free of charge via the Internet at http://pubs.acs.org.

References and Notes

(1) (a) Shin, K.; Xiang, H.; Moon, S. I.; Kim, T.; McCarthy, T. J.; Russell, T. P. *Science* **2004**, *306*, 76. (b) Bucknall, D. G.; Anderson, H. L. *Science* **2003**, *302*, 1904−1905. (c) Hamley, I. W. *The Physics of Block Copolymers*; Oxford: Oxford, U.K., 1999. (d) Muthukumar, M.; Ober, C. K.; Thomas, E. L. *Science* **1997**, *277*, 1225−1232. (e) Bates, F. S.; Fredickson, G. H. *Annu. Rev. Phys. Chem.* **1990**, *41*, 525−557. (f) Lodge, T. P. *Macromol. Chem. Phys.* **2003**, *204*, 265−273.

(2) (a) Krausch, G.; Magerle, R. *Adv. Mater.* **2002**, *14*, 1579−1583. (b) Kataoka, K.; Harada, A.; Nagasaki, Y. *Adv. Drug Delivery Rev.* **2001**, *47*, 113−131.

(3) Buzza, D. M. A.; Fzea, A. H.; Allgaier, J. B.; Young, R. N.; Hawkins, R. J.; Hamley, I. W.; McLeish, T. C. B.; Lodge, T. P. *Macromolecules* **2000**, *33*, 8399−8414.

(4) (a) Bates, F. S.; Fredrickson, G. H. *Phys. Today* **1999**, *52*, 32−38. (b) Abetz, V.; Stadler, R. *Macromol. Symp.* **1997**, *113*, 19−26.

(5) (a) Goldacker, T.; Abetz, V. *Macromol. Rapid Commun.* **2000**, *21*, 16−34. (b) Goldacker, T.; Abetz, V.; Stadler, R.; Erukhimovich, I.; Leibler, L. *Nature (London)* **1999**, *398*, 137−139.

(6) Stupp, S. I.; LeBonheur, V.; Walker, K.; Li, L. S.; Huggins, K. E.; Keser, M.; Amstutz, A. *Science* **1997**, *276*, 384−389. (b) Chen, J. T.; Thomas, E. L.; Ober, C. K.; Mao, G.-p. *Science* **1996**, 343−346.

(7) (a) Adams, J.; Sänger, J.; Tefehne, C.; Gronski, W. *Macromol. Rapid Commun.* **1994**, *15*, 879−886. (b) Adams, J.; Gronski, W. *Macromol. Rapid Commun.* **1989**, *10*, 553−557.

(8) Zhang, A.; Shu, L.; Bo, Z.; Schlüter, A. D. *Macromol. Chem. Phys.* **2003**, *204*, 328−329.

(9) (a) Cho, B.-K.; Jain, A.; Gruner, S. M.; Wiesner, U. *Science* **2004**, *305*, 1598−1601. (b) Hadjichristidis, N.; Pitsikalis, M.; Pispas, S.; Iatrou, H. *Chem. Rev.* **2001**, *101*, 3747−3792. (c) Pitsikalis, M.; Pispas, S.; Mays, J. W.; Hadjichristidis, N. *Adv. Polym. Sci.* **1998**, *135*, 1−137. (d) Roovers, J.; Comanita, B. *Adv. Polym. Sci.* **1999**, *142*, 179−228.

(10) (a) Gitsov, I. *Linear-Dendritic Block Copolymers. Synthesis and Characterization*; Newkome, G. R.; Advances in Dendritic Macromolecules 5; Elsevier Science: Amsterdam, 2002; Chapter 2, pp 45−87. (b) Gitsov, I.; Lambrych, K. L.; Ivanova, P. T.; Lewis, S. *Polym. Mater. Sci. Eng.* **2001**, *84*, 926. (c) Chang, Y.; Kwon, Y. C.; Lee, S. C.; Kim, C. *Macromolecules* **2000**, *33*, 4496−4500. (d) Iyer, J.; Fleming, K.; Hammond, P. T. *Macromolecules* **1998**, *31*, 8757−8765. (e) Leduc, M.; Hayes, W.; Fréchet, J. M. J. *J. Polym. Sci., Part A: Polym. Chem.* **1998**, *36*, 1−10. (f) van Hest, J. C. M.; Delnoye, D. A. P.; Baars, M. W. P. L.; van Genderen, M. H. P.; Meijer, E. W. *Science* **1995**, *268*, 1592−1595. (g) Chapman, T. M.; Hillyer, G. L.; Mahan, E. J.; Shaffer, K. A. *J. Am. Chem. Soc.* **1994**, *116*, 11195−11196. (h) Gitsov, I.; Ivanova, P. T.; Fréchet, J. M. J. *Macromol. Rapid Commun.* **1994**, *15*, 387−393.

(11) (a) Duan, X. X.; Yuan, F.; Wen, X. J.; Yang, M.; He, B.; Wang, W. *Macromol. Chem. Phys.* **2004**, *205*, 1410−1417. (b) Johnson, M. A.; Iyer, J.; Hammond, P. T. *Macromolecules* **2004**, *37*, 2490−2501. (c) Johnson, M. A.; Santini, C. M. B.; Iyer, J.; Satija, S.; Ivkov, R.; Hammond, P. T. *Macromolecules* **2002**, *35*, 231−238. (d) Pochan, D. J.; Pakstis, L.; Huang, E.; Hawker, C.; Vestberg, R.; Pople, J. *Macromolecules* **2002**, *35*, 9239−9242. (e) Mackay, M. E.; Hong, Y.; Jeong, M.; Tande, B. M.; Wagner, N. J.; Hong, S.; Gido, S. P.; Vestberg, R.; Hawker, C. J. *Macromolecules* **2002**, *35*, 8391−8399. (f) Román, C.; Fischer, H. R.; Meijer, E. W. *Macromolecules* **1999**, *32*, 5525−5531. (g) Gitsov, J.; Fréchet, J. M. J. *Macromolecules* **1993**, *24*, 6536−6546.

(12) A preliminary account of a fraction of this work has been given in the context of two preprints: (a) Pusel, T.; Frey, H.; Lee, Y. U.; Jo, W. H. *Polym. Mater. Sci. Eng.* **2001**, *84*, 730. (b) Garcia Marcos, A.; Pusel, T.; de Juan de Castro, B.; Geppert, S.; Thomann, R.; Gronski, W.; Frey, H. *Polym. Prepr.* **2003**, *44*, 534−541.

(13) Sänger, J.; Tefehne, C.; Lay, R.; Gronski, W. *Polym. Bull.* **1996**, *36*, 19−26.

(14) This monomer was first used by Möller et al.: Drohmann, C.; Möller, M.; Gorbatsevich, O. B.; Muzafarov, A. M. *J. Polym. Sci., Polym. Chem.* **2000**, *38*, 741−751.

(15) (a) Kim, C.; Kang, S. *J. Polym. Sci., Part A: Polym. Chem.* **2000**, *38*, 724−729. (b) Britcher, L. G.; Kehoe, D. C.; Matisons, J. G.; Swincer, A. G. *Macromolecules* **1995**, *28*, 3110−3118. (c) Lewis, L. N. *J. Am. Chem. Soc.* **1990**, *112*, 5998−6004. (d) Chalk, A. J.; Harrod, J. F. *J. Am. Chem. Soc.* **1965**, *87*, 16−21.

(16) (a) Speier, J. L. *Adv. Organomet. Chem.* **1979**, *17*, 407. (b) Karstedt, B. D. U.S. Patent 3,775,452, 1973.

(17) (a) Hanselmann, R.; Hölter, D.; Frey, H. *Macromolecules* **1998**, *31*, 3790−3801. (b) Radke, W.; Litvinenko, G.; Müller, A. H. E. *Macromolecules* **1998**, *31*, 239−248.

(18) Guo, X.; Rempel, G. L. *Macromolecules* **1992**, *25*, 883−886.

(19) Onopchenko, A.; Sabourin, E. T. *J. Org. Chem.* **1987**, *52*, 4118−4121.

(20) Brook, M. A. *Silicon in Organic, Organometallic and Polymer Chemistry*; Wiley: New York, London, 2000.

(21) (a) Pochan, D.; Gido, S. P.; Pispas, S.; Mays, J. W.; Ryan, A. J.; Fairclough, J. P. A.; Hamley, I. W.; Terrill, N. J. *Macromolecules* **1996**, *29*, 5091−5098. (b) Pochan, D.; Gido, S. P.; Pispas, S.; Mays, J. W. *Macromolecules* **1996**, *29*, 5099−5105.

(22) Hadjichristidis, N.; Tselikas, Y.; Iatrou, H.; Efstratiadis, V.; Avgeropoylos, A. *J. Macromol. Sci.—Pure Appl. Chem.* **1996**, *10*, 1447−1457.

(23) Barriau, E.; Garcia-Marcos, A.; Kautz, H.; Frey, H. *Macromol. Rapid Commun.* **2005**, *11*, 862−868.

MA051526C